Draft version May 26, 2009
Preprint typeset using LaTeX style emulateapj v. 10/09/06

REVISITING THE ROLE OF M31 IN THE DYNAMICAL HISTORY OF THE MAGELLANIC CLOUDS

Nitya Kallivayalil[1,2]
MIT Kavli Inst. for Astrophysics & Space Research, 70 Vassar Street, Cambridge, MA 02139

Gurtina Besla
Harvard-Smithsonian Center for Astrophysics, 60 Garden Street, Cambridge, MA 02138

Robyn Sanderson
MIT Kavli Inst. for Astrophysics & Space Research, 70 Vassar Street, Cambridge, MA 02139

Charles Alcock
Harvard-Smithsonian Center for Astrophysics, 60 Garden Street, Cambridge, MA 02138
Draft version May 26, 2009

ABSTRACT

We study the dynamics of the Magellanic Clouds in a model for the Local Group whose mass is constrained using the timing argument/two-body limit of the action principle. The goal is to evaluate the role of M31 in generating the high angular momentum orbit of the Clouds, a puzzle that has only been exacerbated by the latest *HST* proper motion measurements. We study the effects of varying the total Local Group mass, the relative mass of the Milky Way and M31, the proper motion of M31, and the proper motion of the LMC on this problem. Over a large part of this parameter-space we find that tides from M31 are insignificant. For a range of LMC proper motions approximately 3σ higher than the mean and total Local Group mass $> 3.5 \times 10^{12} M_{\odot}$, M31 can provide a significant torque to the LMC orbit. However, if the LMC is bound to the MW, then M31 is found to have negligible effect on its motion and the origin of the high angular momentum of the system remains a puzzle. Finally, we use the timing argument to calculate the total mass of the MW-LMC system based on the assumption that they are encountering each other for the first time, their previous perigalacticon being a Hubble time ago, obtaining $M_{\rm MW} + M_{\rm LMC} = (8.7 \pm 0.8) \times 10^{11} M_{\odot}$.

Subject headings: galaxies: evolution – galaxies: kinematics and dynamics – galaxies: interactions – Local Group – Magellanic Clouds

1. INTRODUCTION

The three-dimensional velocities of the Magellanic Clouds, from proper motion measurements using *HST's* Advanced Camera for Surveys (ACS) and a sample of background QSOs (Kallivayalil et al. 2006a,b, hereafter K1 and K2; see also Piatek et al. 2008, Kallivayalil et al. 2009), are ~ 100 km s^{-1} higher than those used in past theoretical modeling of the Magellanic Stream (MS) and, for the LMC, now approach the escape velocity of the Milky Way (MW). Consequently, as shown by Besla et al. (2007), in a ΛCDM-based model for the MW the Clouds, assuming they form a bound system, are likely on their first passage. This claim has re-ignited the discussion about the origin of the Clouds. Did they form in the outer regions of the Local Group or as satellite galaxies of the MW? Proposals for the latter, i.e., that bind the Clouds to the MW, include the explicit use of smaller velocities, for example, by giving the LMC & SMC a common halo (Bekki 2008) as well as Modified Newtonian Dynamics (MOND) gravity (Wu et al. 2008). A recent study by Shattow & Loeb (2009) argues that the past orbit of the LMC is naturally confined within the virial radius of the MW if a $\sim 14\%$ increase in the MW circular velocity (Reid & Brunthaler 2004; Reid et al. 2009) is taken in combination with the lower end of the allowed proper motion error-space.

Apart from uncertainties in the MW potential, other puzzles remain, such as the high angular momentum of the LMC system (e.g. Fich & Tremaine 1991; Gott & Thuan 1978). Even with the modest values for transverse velocity ($\sim$ 100 km s^{-1}) and apogalacticon distance (200 kpc) used in past MS models, a mass of $L_{\rm LMC} = 2 \times 10^{10} M_{\odot}$ gives the following for the orbital angular momentum, $L_{\rm LMC}$, of the LMC: $L_{\rm LMC} \sim M_{\rm LMC} R_{\rm LMC} V_{\rm LMC} \sim 4 \times 10^{14} M_{\odot}$kpc km s^{-1} . This is equivalent to the spin angular momentum of the Galactic disk, $L_{\rm disk} \sim (2/3) M_{\rm disk} R_{\rm disk} V_0 \sim 4 \times 10^{14} M_{\odot}$kpc km s^{-1} , with standard values of $M_{\rm disk} = 2 \times 10^{11} M_{\odot}$, $R_{\rm disk} = 15$ kpc and $V_0 = 220$ km s^{-1} (Sawa & Fujimoto 2005). Since the LMC is in a roughly polar orbit, these angular momenta make right angles to each other.

This problem has seen many past iterations: Besla et al. (2007) show that the LMC may be on a parabolic orbit, and hence the 'angular momentum problem' is moot. However, in this case an explanation of why the LMC is moving so quickly and on such a different orbit from the other satellites is warranted. For example, Fich & Tremaine (1991) comment that the maximum

[1] Pappalardo Fellow
[2] nitya@mit.edu

line-of-sight velocity of the MS (-410 km s^{-1} ; Brüns et al. 2005) is not only higher than that of the Clouds themselves (262 km s^{-1}) but also higher than any MW satellite within 200 kpc. Morphological studies of the satellite populations of the MW and M31 arrive at a similar impasse. Van den Bergh (2006) argues that the fact that the Clouds are gas-rich dIrr galaxies and yet occupy the small Galactocentric distances usually dominated by dSph galaxies may be accounted for by assuming that they are interlopers that were originally formed in the outer reaches of the Local Group.

Raychaudhury & Lynden-Bell (1989) contended that M31 was close enough to the LMC in its early orbital history to cause a significant tide, and that this tide was oriented such as to generate the high orbital angular momentum of the Clouds. It is worth noting here that their analysis was done in the context of external tides on the MW-M31 system from more distant galaxies. Building on this theory, Shuter (1992) and Byrd et al. (1994) considered the possibility that the Clouds underwent a close encounter with M31 having only recently been captured by the MW. Given our new velocities it is especially pertinent to not consider the LMC-SMC-MW system in isolation and to explore whether the Clouds may have been subject to external torques before entering the environs of the MW. We revisit this classic problem of quantifying the torque provided by M31 using the framework of the timing argument/two-body limit of the least action principle, given two new pieces of information: the new proper motions for the Clouds *and* a new transverse velocity estimate for M31 from satellite velocities (van der Marel & Guhathakurta 2008; hereafter VG08).

Shattow & Loeb (2009) also included the effect of M31 in their analysis of whether the LMC is bound to the MW. We confirm the results in § 4 of their paper but take a different approach here. Within the framework of the timing argument/two-body limit of the least-action principle, could M31 have generated the high transverse velocities of the Clouds? There are 4 main effects on the Clouds' orbits that bear exploring: 1) the effect of total Local Group mass, M_{tot}; 2) the effect of $f = M_{\rm M31}/M_{\rm MW}$; 3) the effect of M31 proper motion; and 4) the effect of varying the proper motion of the LMC. There is a large range in values for M_{tot} because this is a quantity that cannot be directly measured without modeling. Various methods give a range of $2 \times 10^{12} - 5.6 \times 10^{12} M_{\odot}$ (Kochanek 1996; Wilkinson & Evans 1999; Klypin et al. 2002; VG08). The quantity f is also hard to constrain observationally and we look at a range of values from 0.8 - 2.0 (Einasto & Lynden-Bell 1982; Evans & Wilkinson 2000; Klypin et al. 2002; VG08). Recent VLBA measurements might favor f closer to unity (Reid et al. 2009). The proper motion of M31 has not been directly measured, but as mentioned above, indirect estimates exist and indicate that it is small (VG08). We investigate the full range of values from the literature. Finally, the proper motion of the LMC is the only observationally well-constrained quantity in this analysis (K1) and we test the whole error-space using a Monte-Carlo distribution.

The primary goal is to assess whether the inclusion of M31 in the equations of motion of the Clouds can generate a significant torque on the L/SMC orbit. In addition, we keep track of the magnitude of the relative tidal force on the LMC from the MW and M31 to quantify whether there are orbits in which the M31 tide is higher. The tide is calculated simply via a double radial differentiation of the potential at the location of the L/SMC. While the locations of the center-of-mass of the L/SMC are allowed to move under the influence of the two more massive bodies, the potential shapes in all simulations are kept fixed. Motivated by the findings of this analysis, we apply the timing argument to the MW and LMC, assuming that the LMC is on its first passage with the previous perigalacticon being a Hubble time, t_H, ago, to calculate the mass of the MW.

In most of the subsequent analysis we present results only for the LMC and intend our conclusions to be representative of the LMC-SMC system as a whole. It remains a possibility that the Clouds are not in a binary system (K2; Piatek et al. 2008). We do not explicitly investigate this further as it is still possible to find a binary orbit in the error space of the SMC for every given LMC orbit. Also, a chance three-body interaction (MW-LMC-SMC) seems highly unlikely. It has been speculated, for instance, that the Clouds are members of a small subgroup that was captured by the Local Group (Metz et al. 2009), or that fell into the MW at late times (D'Onghia & Lake 2009). Given their mass ratio ($\sim 10:1$) the SMC is not expected to play a major role in shaping the orbit of the LMC. We thus carry out the analysis assuming that the orbital path of the Clouds will be dependent on that of the LMC, but we do include the perturbative effect of the SMC on the LMC given the SMC mean velocity in all our calculations (note, however, that this is an orbit in which the Clouds are unbound to each other). We await smaller proper motion errors for the SMC (see § 4) to lift these assumptions.

In § 2 we recount briefly the work on the relative motion of the MW and M31 and use this as the motivation for our Local Group model and methods. In § 3 we present results including changes to the orbital history of the LMC given these new models. We also present the results for MW mass. We conclude in § 4.

2. A MODEL FOR THE LOCAL GROUP

2.1. *The Relative Motion of the Milky Way and M31*

The Local Group is thought to be decoupled from the cosmological expansion and gravitationally bound. This is supported by the fact that its two major constituents, the MW and M31, are seen to be approaching each other with a radial velocity of ~ 117 km s^{-1} (Binney & Tremaine 1987). The tangential motion of M31 has not been directly measured, but indirect estimates (VG08; Loeb et al. 2005; Peebles et al. 2001) indicate that this tangential motion is small, and thus support the assumption that the Local Group is bound.

Some simple dynamical arguments about the the Local Group can be made based on known facts. In 1959, Kahn & Woltjer proposed the 'timing argument', in which the MW and M31 first moved apart due to general cosmological expansion, subsequently reversed paths and are now falling into each other under their own gravitational attraction, their motions being governed by Newtonian dynamics. Assuming a zero angular momentum orbit (zero tangential motion) and the known current separation and radial velocity, the timing argument requires a mass in the Local Group $> 3 \times 10^{12} M_{\odot}$ to fulfill this

trajectory. An alternative explanation would be that the MW and M31 are accidentally passing by, but if the galaxies have moved at a constant speed for a Hubble time, their separation would have changed only by ~ 117 km s^{-1} $/H_0 \sim 1.6$ Mpc, i.e., less than the distance to the next largest galaxy. So this is not a promising alternative (Peebles 1993).

A more sophisticated treatment of the dynamics of the Local Group, pioneered by Peebles (1989; 1990; Shaya et al. 1995; Peebles et al. 2001), involves using the principle of least-action to calculate orbital solutions from incomplete phase-space information by assuming homogeneity of the early universe (see also Goldberg & Spergel 2000; Goldberg 2001). Note, however, that the two-body limit to this solution is equivalent to the timing argument, since the equation of relative motion has the same form as the cosmological acceleration equation in the case of the evolution of a homogeneous, isotropic mass distribution (Peebles 1993).

The timing argument has been investigated and applied widely in the literature (Mishra 1985; Raychaudhury & Lynden-Bell 1989; Kroeker & Carlberg 1991; Goldberg 2001). Two recent extensions of the formalism bear further comment: (1) Chernin et al. (2009) include the antigravity effect of dark energy in the Kahn-Woltjer model and find a larger Local Group mass than in traditional methods of $4.5 \times 10^{12} M_\odot$; (2) VG08 applied the timing argument to obtain a total mass for the Local Group, after first deducing a transverse velocity for M31 from satellite velocities. The methods they use for the latter are a statistical analysis of the line-of-sight velocities of 17 M31 satellites, a study of the proper motions of two satellites M33 and IC 10 (from Brunthaler et al. 2005, 2007), and an analysis of the line-of-sight velocities of 5 galaxies near the Local Group turn-around radius. A full Monte Carlo analysis of all the uncertainties involved produces a value of $V_{\rm tan} = 41.7$ km s^{-1} for the median of the probability distribution of the Galactocentric tangential velocity of M31, with 1σ confidence interval $V_{\rm tan} \leq 56$ km s^{-1} (thus the radial orbit applied by Kahn & Woltjer is allowed in their solution). The inferred 1σ confidence interval around the median Local Group mass obtained from application of the timing argument is $5.58^{+0.85}_{-0.72} \times 10^{12} M_\odot$.

While this mass is consistent with most applications of the timing argument, it is on the high end of what is predicted from ΛCDM motivated galaxy models (Klypin et al. 2002; Li & White 2008). Using theoretical constraints to narrow the large space of solutions allowed by uncertainties in satellite velocities and in halo extent, the Klypin et al. models for M31 and the MW have a favored total mass of $2.6 \times 10^{12} M_\odot$ (with a maximum upper-limit of roughly twice this amount). The reason for the discrepancy is unclear, the general wisdom being that the timing argument provides too simplistic a view of mass-accretion. However, some studies (Kroeker & Carlberg 1991) have investigated its accuracy in a cosmological context and found it an adequate approximation to the true mass.

Our aim is not to build a 'true' Local Group but rather to investigate maximal M31 models, i.e., models in which M31 can hope to generate large torques on the LMC orbit. Thus the timing argument provides a natural framework in which to carry out these investigations.

2.2. *Methods*

We estimate the effect of M31 by building on the timing argument and considering some representative cases of the entire paramater-space: we vary the total Local Group mass, M_{tot}, from $2.6 - 6 \times 10^{12} M_\odot$ and also consider two cases for the proper motion of M31 - the mean value from VG08 as well as a radial orbit. Table 1 summarizes the quantities varied, the step-size of the variation or error-space explored. We solve the two-body problem for the motion of M31 relative to the MW in the same MW-centered coordinate system (X, Y, Z) that we used for the Clouds (see K1 and van der Marel et al. 2002) and then include M31's potential in the equations of motion for the Clouds, knowing the distance between the Clouds and M31 at every time-step. In solving for the radial orbit we assume a distance modulus of 24.47 (McConnachie et al. 2005; Ribas et al. 2005), a radial velocity (of M31 relative to the MW) of -117 km s^{-1} (Binney & Tremaine 1987) and a current location for M31 of (RA = 10.68°, Dec = 41.27°, J2000.0). For the non-radial case we simply adopt the six phase-space parameters supplied by VG08. Given the adopted initial conditions, we are free to choose the total mass (represented here as $\mu = G(M_{\rm M31} + M_{\rm MW})$) so as to specify the time in the past at which the MW and M31 were co-located. Figure 1 shows the resulting motion of M31 with respect to the MW in our Galactocentric frame for a few different values of μ/G and a radial orbit.

As expected, orbits with total mass $\mu/G < 3 \times 10^{12} M_\odot$ do not 'turn around' within t_H. In Figure 1 we show that as μ increases, the turn around time decreases; the dotted line shows the past orbit for $\mu/G = 2.6 \times 10^{12} M_\odot$, the solid line shows the case of $\mu/G = 4.6 \times 10^{12} M_\odot$ and the dashed line for $\mu/G = 5.2 \times 10^{12} M_\odot$. The non-radial orbits have the same qualitative behavior with mass and we do not plot them here. As in VG08, all quantities are found to vary monotonically with the tangential velocity of M31: larger values of tangential velocity lead to larger values of total mass, the period of the orbit and the pericentric distance. We show the full Hubble time evolution of the orbit in Figure 1 simply as a heuristic exercise. There is little value in extending our static analysis to significantly earlier times than 5 Gyr ago since stellar ages imply that the Galactic disk (and presumably the halo) had not been fully assembled at $z \gtrsim 2$ (Wyse 2007; Cox & Loeb 2008).

Once the mutual separation of M31 and MW is known it is easy to introduce a potential term for M31 in the equations of motion for the L/SMC:

$$\frac{d^2 \mathbf{r}_L}{dt^2} = \begin{array}{l} \frac{\partial}{\partial \mathbf{r}_L}[\phi_S(\mid \mathbf{r}_L - \mathbf{r}_S \mid) + \\ \phi_{\rm MW}(\mid \mathbf{r}_L \mid) + \phi_{\rm M31}(\mid \mathbf{r}_L - \mathbf{r}_{M31} \mid)] + \frac{\mathrm{F}_L}{M_L}, \end{array} \quad (1)$$

where $\mathbf{r}_L$ is the Galactocentric distance of the LMC, $\mathbf{r}_S$ that of the SMC and $\mathbf{r}_{M31}$ that of M31. ϕ_S is the potential of the SMC, $\phi_{\rm MW}$ is the potential of the MW and $\phi_{\rm M31}$ is that of M31. F_L is the dynamical friction on the LMC orbit and M_L is the mass of the LMC. There is an equivalent equation for the SMC. In this model for the Local Group, the MW and M31 are both approximated as isothermal spheres with $\phi_{\rm MW,M31}(r) = -V_0^2 \ \ln r$, $V_{0,\rm MW} = 220$ km s^{-1} and $V_{0,\rm M31} = 250$ km s^{-1} (Loeb et al. 2005). To be consistent with the total mass used

in our 2-body formulation we introduce a cut-off radius, r_h, outside which the density drops to zero (see van der Marel et al. 2002):

$$\rho = \begin{cases} V_0^2/4\pi G r^2, & \text{if } r \leq r_h, \\ 0, & \text{if } r > r_h. \end{cases} \quad (2)$$

The enclosed mass is:

$$M(r) = \begin{cases} rV_0^2/G, & \text{if } r \leq r_h, \\ r_h V_0^2/G \equiv M_{\rm tot}, & \text{if } r > r_h. \end{cases} \quad (3)$$

The LMC and SMC are represented using Plummer models:

$$\phi_{L,S}(r) = GM_{L,S}/[(\mathbf{r} - \mathbf{r}_{L,S})^2 + K_{L,S}^2]^{1/2}, \quad (4)$$

with effective radii (K_L, K_S) of 3 and 2 kpc, and masses (M_L, M_S) of $2 \times 10^{10} M_\odot$ and $3 \times 10^9 M_\odot$, respectively. The final term, $\frac{\rm F_L}{M_L}$, accounts for dynamical friction on the LMC orbit resulting from its motion through the MW dark halo, for which we use the Chandrasekhar formula (Binney & Tremaine 1987):

$$F_{L,S} = -\frac{4\pi G^2 M_{L,S}^2 \ln(\Lambda)\rho(r_{L,S})}{v_{L,S}^3} \left\{ [\mathrm{erf}(X) - \frac{2X}{\sqrt{\pi}} e^{-X^2}] \mathbf{v}_{L,S} \right\}, \quad (5)$$

where $X = v_{L,S}/V_{0,\rm MW}$ and $\rho(r_{L,S})$ is the density of the MW halo at the Galactocentric distance of the L/SMC. The strength of this force depends on the mass of the L/SMC, and since we are integrating backwards in time from the current positions and velocities, the sign of the dynamical friction term is that of acceleration (see Figure 2). Our results do not depend sensitively on the form of this drag because as shown in § 3.1 it does not alter the L/SMC orbit in such a way as to bring them significantly closer to M31 in the past. Our conclusions don't change even if it is ignored. Further, we do not include dynamical friction from M31 in our calculations because, as discussed in the next section, the LMC's closest approach to M31 in the past 5 Gyr is roughly 500 kpc. Thus dynamical friction from M31 is negligible.

3. RESULTS

3.1. *LMC Orbits*

We use a Monte Carlo scheme to randomly draw 20,000 LMC proper motion components from the errors in K1. From these initial values we allow the LMC orbit to propagate backward in time in the Local Group model described in § 2. The SMC proper motion is kept fixed at its mean value (K2). We keep track of the orbits that take the LMC closest to and furthest from M31.

As laid out in the introduction, we explore the effects of 1) M_{tot}; 2) f; 3) M31 proper motion; and 4) LMC proper motion on the past orbital history of the Clouds. It was found that as M_{tot} increases, the orbital period and apogalacticon of the LMC orbit is smaller, as one might expect. However, M_{tot} does not have any direct bearing on the relative importance of M31 in the LMC's past. The question becomes, given a value of M_{tot}, what are the salient changes to the LMC orbit from varying f, the LMC proper motion and M31's proper motion? The largest change to the orbit comes from varying the LMC proper motion, followed by changes in f. The proper motion of M31, by contrast, does not dramatically alter the picture. It acts much like M_{tot} : larger values of M31 proper motion require larger values of M_{tot} to fulfill the trajectory of the timing argument. The currently accepted error-space of M31's proper motion does not alter its relative distance to the LMC dramatically. However, the proper motion of the LMC does.

We summarize the results in Figure 2. The black solid line shows the orbit with $M_{tot} = 5.6 \times 10^{12} M_\odot$, $f = 1$, mean LMC proper motion and mean M31 proper motion (from VG08). This can be compared to the black dotted line which is the orbit obtained in a MW-only Local Group (with $M_{\rm MW} = 2.8 \times 10^{12} M_\odot$). Note that this MW differs from our 'infinite mass' fiducial model in K2 in that it is modeled with a cut-off radius and thus fixed total mass. We realize this is a larger MW mass than indicated by either observations or ΛCDM modeling but emphasize that we are trying to understand the relative importance of M31 in LMC dynamics for which M_{tot} itself turns out to be unimportant. Varying M_{tot} pushes the LMC orbit to larger or shorter period, but the qualitative picture remains. As for the choice of mass distribution, we contend that the treatment of M31 as an isothermal sphere is adequate because, as described below, the LMC does not come closer than $\sim$ 500 kpc. As for the choice of mass distribution for the MW, we showed in Figure 8 in Besla et al. (2007) that the trajectories of the LMC line up in projection regardless of whether an isothermal sphere or NFW (Navarro et al. 1996; 1997) profile are used. Thus, replacing the isothermal spheres here with NFW models is equivalent to looking at lower values of M_{tot}: the LMC would effectively escape sooner from the MW in the past and with lower velocity, but at the same time, M31 would be further away.

The dashed pink lines in Figure 2 mark the boundaries of $f = 0.8$ (minimal M31 model) and $f = 2.0$ (maximal M31 model) for fixed M_{tot}. The green lines enclose the space of solutions given by LMC proper motion: the LMC orbits with closest approach to M31 have the mean western LMC proper motion, μ_W, in the range of $\mu_W - (> 3\sigma)$, while the furthest orbits are for $\mu_W + (> 3\sigma)$. These also naturally correspond to unbound and bound orbits to the MW, respectively. The northern component of the proper motion, μ_N, does not affect the trajectory as dramatically (see Figure 3).

Within a period of 5 Gyr, the closest orbits bring the LMC within $\sim$ 500 kpc of M31, while the furthest orbits come within $\sim$ 770 kpc. Since the distance to M31 is relatively large throughout the duration of our calculations and tides drop off as r^{-3} it seems unlikely that M31 would have a pronounced effect on the orbits of the Clouds, and this is the case for most of the parameter-space that we search. However, for a range of LMC proper motions $\mu_W - (> 3\sigma)$ the torque provided by M31 can be significant. In Figure 3 we show the closest distance to M31 reached by the LMC as a function of the LMC's μ_W, μ_N, and their corresponding error circles. The black dots are for $M_{tot} = 2.6 \times 10^{12} M_\odot$, the green dots for $M_{tot} = 3.5 \times 10^{12} M_\odot$, the blue dots for $M_{tot} = 4.6 \times 10^{12} M_\odot$ and the pink dots for $M_{tot} = 5.6 \times 10^{12} M_\odot$. The M31 tangential velocity is that of VG08. There is a clear dependence on μ_W but not on μ_N. For the case of $-2.3 < \mu_W < -2.2$ mas yr^{-1} and $M_{tot} > 3.5 \times 10^{12} M_\odot$, the final relative velocity between the LMC and M31 is smaller than the escape velocity

of M31, but the relative distance is larger than $r_{h,\rm M31}$. As M_{tot} increases the value of μ_W must also in general increase for this to be the case. Varying f broadens the distributions in Figure 3 (*left* panel) by decreasing (high f) or increasing (low f) the distances of closest approach.

Figure 4 shows the past orbits of the Clouds in aitoff projection, centered on the MW. The pink triangle, blue diamond and red square mark the current positions of the LMC, SMC and M31 respectively. Again, the M31 tangential velocity is that of VG08. We do not show the M31 orbit here because, as in the case of the radial orbit, the trajectory in aitoff projection is roughly constant. For a given M_{tot} the pink solid line shows the LMC orbit trajectory that takes it closest to M31, while the pink dashed lines show the corresponding furthest orbits. The blue dotted line shows the mean SMC orbit for reference. As seen in Figure 2, M31 does provide a small amount of tidal pull on the LMC orbit compared to a MW-only Local Group even for the mean velocities. However, M31 can only *alter* the orbit of the LMC if the LMC is moving roughly $3-4\sigma$ faster than we think, i.e., it is not bound to the MW at all. For these cases the tidal influence of M31 is larger than that of the MW (solid pink line) and the final relative velocity between the LMC and M31 is lower than the escape velocity of M31, even though the relative distance is larger than $r_{h,\rm M31}$. If we do allow our calculations of these particular orbits to run for t_H (not shown here), the LMC eventually becomes bound to M31. However, accounting for the hierarchical build-up of the Local Group, this analysis becomes inaccurate past 5 Gyr. The plot looks qualitatively the same when varying M_{tot}.

Figure 5 quantifies the strength of the tidal force exerted on the LMC by the MW and M31 as a function of time. The tidal force is calculated by twice differentiating the gravitational potential of the galaxy in question at the position of the LMC, even though strictly the tidal field is a traceless tensor that requires tangential derivatives as well. The radial derivative is proportional to the tide only for a perturbed body of constant size (see Gardiner & Noguchi 1996) but is instructive here given our methods. Figure 5 (*left*) shows the relative tidal forces on the LMC orbit that is furthest from M31 (bound to the MW), and on the right for the LMC orbit that comes closest to M31 (unbound to the MW). The dotted line shows the tidal force exerted by the MW and the dashed lines shows the same for M31. The M31 tide takes over for orbits moving 3σ faster than the mean, but is insignificant for lower values of LMC velocity.

3.2. *MW Mass*

If the LMC is indeed on its first passage about the MW then we can use the timing argument to estimate the total mass of the LMC-MW system. This is not strictly a correct application of the timing argument because for a small galaxy such as the LMC, the details of the neighboring mass distribution become important and cannot be treated as homogeneous and isotropic. Even so, it is instructive to see what kind of limits the timing argument places on the mass of the MW given the assumption that the LMC and MW are encountering each other for the first time. Since the current position and velocity of the LMC relative to the MW is known, this specifies the semi-major axis of the relative orbit via the cubic equation

$$2n^2a^3 - n^2 r_L a^2 - r_L v_L^2 = 0, \qquad (6)$$

where a is the semi-major axis, $n = 2\pi/T$ is the mean motion, and r_L and v_L are the position and velocity at time zero. If $T = t_{\rm H} = 13.7$ Gyr (Hinshaw et al. 2008), we can solve uniquely for $\mu = G(M_{\rm MW} + M_{\rm LMC}) = n^2a^3$. A Monte-Carlo analysis of the errors in LMC velocity gives:

$$M_{\rm MW} + M_{\rm LMC} = (8.7 \pm 0.8) \times 10^{11} M_\odot, \qquad (7)$$

which is in good agreement with ΛCDM-based estimates for the mass of the MW (e.g., Klypin et al. 2002). It is lower than recent observational estimates based on VLBA measurements by about a factor of 2 (Reid et al. 2009).

4. CONCLUSIONS

We have studied the past orbital histories of the Clouds in a model for the Local Group whose properties are constrained using the timing argument. This study has been motivated by the substantial increase in the tangential velocity of the LMC (K1; Piatek et al. 2008; Kallivayalil et al. 2009) and thus the possibility that the LMC is on its first passage about the MW (Besla et al. 2007), as well as a new assessment of the tangential velocity of M31 (VG08). The timing argument provides a natural framework within which to test the effect of 'maximal' M31 models on the past orbit of the LMC. The goal is to evaluate whether, as in Raychaudhury & Lynden-Bell (1989) for instance, tidal torques exerted by M31 are important for the LMC.

We investigate the effects of M_{tot}, $f = M_{M31}/M_{MW}$, M31 proper motion and LMC proper motion. We find that M_{tot} and M31 proper motion both act in the same way : larger values of M31 tangential velocity lead to larger values of M_{tot}, period and pericentric distance of the MW-M31 orbit. These in turn affect the period and peri/apogalactic distances of the MW-LMC orbit, but within the accepted error-space, M31 proper motion does not significantly affect the trajectory of the LMC orbit. M_{tot} does affect the trajectory of the orbit if M31 is sufficiently massive ($M_{tot} > 3.5\times10^{12} M_\odot$) and if the western component of the LMC proper motion, μ_W is increased by roughly 3σ. The amount of this increase depends on M_{tot}. However, for the rest of the explored parameter-space, the influence of M31 is negligible. Furthermore, it is unlikely that we have underestimated the proper motion of the LMC by this amount, and thus conclude that the M31 tide is likely insufficient in generating the high angular momentum of the LMC orbit. In other words, the angular momentum problem remains.

Finally, motivated by the fact that the LMC could be on its first passage about the MW, we calculate the implied MW+LMC mass if they were last co-located a Hubble time ago. A Monte-Carlo analysis of the errors gives: $M_{\rm MW} + M_{\rm LMC} = (8.7 \pm 0.8) \times 10^{11} M_\odot$. Since $M_{\rm MW} >> M_{\rm LMC}$, this quantity is roughly the mass of the MW, and is in good agreement with ΛCDM predictions (e.g., Klypin et al. 2002).

It is clear from this analysis that the large tangential motion of the LMC cannot be easily explained away with manipulations of the Local Group model. Confirming this large motion is a high priority. In Kallivayalil

et al. (2009) we presented an ongoing analysis of the proper motions of the Magellanic Clouds using a third epoch of WFPC2 data centered on background quasars. The results so far as consistent with those presented in K1. At present the RMS error in the position of the quasar is roughly 3 times as large for WFPC2 as for ACS. However, with an improved method to deal with charge-transfer efficiency and magnitude-related effects, and with the increase in time-baseline from 2 to 5 years, we expect final error bars for the proper motions that are smaller by a factor of ~ 2 from K1. This, combined with our understanding of the properties of the MS, will allow us to better constrain the orbit of the Clouds and make more specific predictions as to their origin.

We would like to thank Ed Bertschinger, Paul Schechter and TJ Cox for useful discussions.

REFERENCES

Bekki, K. 2008, ApJ, 684, L87
Besla, G., Kallivayalil, N., Hernquist, L., Robertson, B., Cox, T. J., van der Marel, R. P., & Alcock, C. 2007, ApJ, 668, 949
Binney, J. & Tremaine, S. 1987, Galactic Dynamics, (Princeton: Princeton Univ. Press)
Brüns, C., et al. 2005, A&A, 432, 45
Brunthaler, A., Reid, M. J., Falcke, H., Greenhill, L. J., & Henkel, C. 2005, Science, 307, 1440
Brunthaler, A., Reid, M. J., Falcke, H., Henkel, C., & Menten, K. M. 2007, A&A, 462, 101
Byrd, G., Valtonen, M., McCall, M., & Innanen, K. 1994, AJ, 107, 2055
Chernin, A. D., Teerikorpi, P., Valtonen, M. J., Byrd, G. G., Dolgachev, V. P., & Domozhilova, L. M. 2009, arXiv:0902.3871
Cox, T. J., & Loeb, A. 2008, MNRAS, 386, 461
D'Onghia, E., & Lake, G. 2009, IAU Symposium, 256, 473
Einasto, J., & Lynden-Bell, D. 1982, MNRAS, 199, 67
Evans, N. W., & Wilkinson, M. I. 2000, MNRAS, 316, 929
Fich, M., & Tremaine, S. 1991, ARA&A, 29, 409
Gardiner, L. T., & Noguchi, M. 1996, MNRAS, 278, 191
Goldberg, D. M., & Spergel, D. N. 2000, ApJ, 544, 21
Goldberg, D. M. 2001, ApJ, 550, 87
Gott, J. R., III, & Thuan, T. X. 1978, ApJ, 223, 426
Hinshaw, G., et al. 2008, arXiv:0803.0732
Kahn, F. D., & Woltjer, L. 1959, ApJ, 130, 705
Kallivayalil, N., van der Marel, R. P., Alcock, C., Axelrod, T., Cook, K. H., Drake, A. J., & Geha, M. 2006a, ApJ, 638, 772 (K1)
Kallivayalil, N., van der Marel, R. P., & Alcock, C. 2006b, ApJ, 652, 1213 (K2)
Kallivayalil, N., van der Marel, R. P., Anderson, J., Besla, G., & Alcock, C. 2009, IAU Symposium, 256, 93
Klypin, A., Zhao, H., & Somerville, R. S. 2002, ApJ, 573, 597
Kochanek, C. S. 1996, ApJ, 457, 228
Kroeker, T. L., & Carlberg, R. G. 1991, ApJ, 376, 1
Li, Y.-S., & White, S. D. M. 2008, MNRAS, 384, 1459
Loeb, A., Reid, M. J., Brunthaler, A., & Falcke, H. 2005, ApJ, 633, 894
McConnachie, A. W., Irwin, M. J., Ferguson, A. M. N., Ibata, R. A., Lewis, G. F., & Tanvir, N. 2005, MNRAS, 356, 979
Metz, M., Kroupa, P., Theis, C., Hensler, G., & Jerjen, H. 2009, ApJ, 697, 269
Mishra, R. 1985, MNRAS, 212, 163
Navarro, J. F., Frenk, C. S., & White, S. D. M. 1996, ApJ, 462, 563
Navarro, J. F., Frenk, C. S., & White, S. D. M. 1997, ApJ, 490, 493
Peebles, P. J. E. 1989, ApJ, 344, L53
Peebles, P. J. E. 1990, ApJ, 362, 1
Peebles, P. J. E. 1993, Principles of Physical Cosmology, (Princeton: Princeton Univ. Press)
Peebles, P. J. E., Phelps, S. D., Shaya, E. J., & Tully, R. B. 2001, ApJ, 554, 104
Piatek, S., Pryor, C., & Olszewski, E. W. 2008, AJ, 135, 1024
Raychaudhury, S., & Lynden-Bell, D. 1989, MNRAS, 240, 195
Reid, M. J., & Brunthaler, A. 2004, ApJ, 616, 872
Reid, M. J., et al. 2009, arXiv:0902.3913
Ribas, I., Jordi, C., Vilardell, F., Fitzpatrick, E. L., Hilditch, R. W., & Guinan, E. F. 2005, ApJ, 635, L37
Sawa, T., & Fujimoto, M. 2005, PASJ, 57, 429
Shattow, G., & Loeb, A. 2009, MNRAS, 392, L21
Shaya, E. J., Peebles, P. J. E., & Tully, R. B. 1995, ApJ, 454, 15
Shuter, W. L. H. 1992, ApJ, 386, 101
van den Bergh, S. 2006, AJ, 132, 1571
van der Marel, R. P., Alves, D. R., Hardy, E., & Suntzeff, N. B. 2002, AJ, 124, 2639
van der Marel, R. P., & Guhathakurta, P. 2008, ApJ, 678, 187 (VG08)
Wilkinson, M.I., & Evans, N.W. 1999, MNRAS, 310, 645
Wu, X., Famaey, B., Gentile, G., Perets, H., & Zhao, H. 2008, MNRAS, 386, 2199
Wyse, R. F. G., 2007, in IAU Symposium Vol. 77, Lessons from Surveys of the Galaxy, pp 1036-1046

TABLE 1
PARAMETER-SPACE

Parameter	Values	Step-size	1σ error
M_{tot} ($M_\odot$).....	$2.6 - 6 \times 10^{12}$	0.1×10^{12}	-
f.....	$0.8 - 2.0$	0.1	-
M31 tangential velocity (km s^{-1}).....	0; 42	-	≤ 56
LMC proper motion (μ_N, μ_W) (mas yr^{-1})	0.44, -2.03	Monte Carlo dist.	0.05, 0.08
SMC proper motion (μ_N, μ_W) (mas yr^{-1})	-1.17, -1.16	-	Fixed

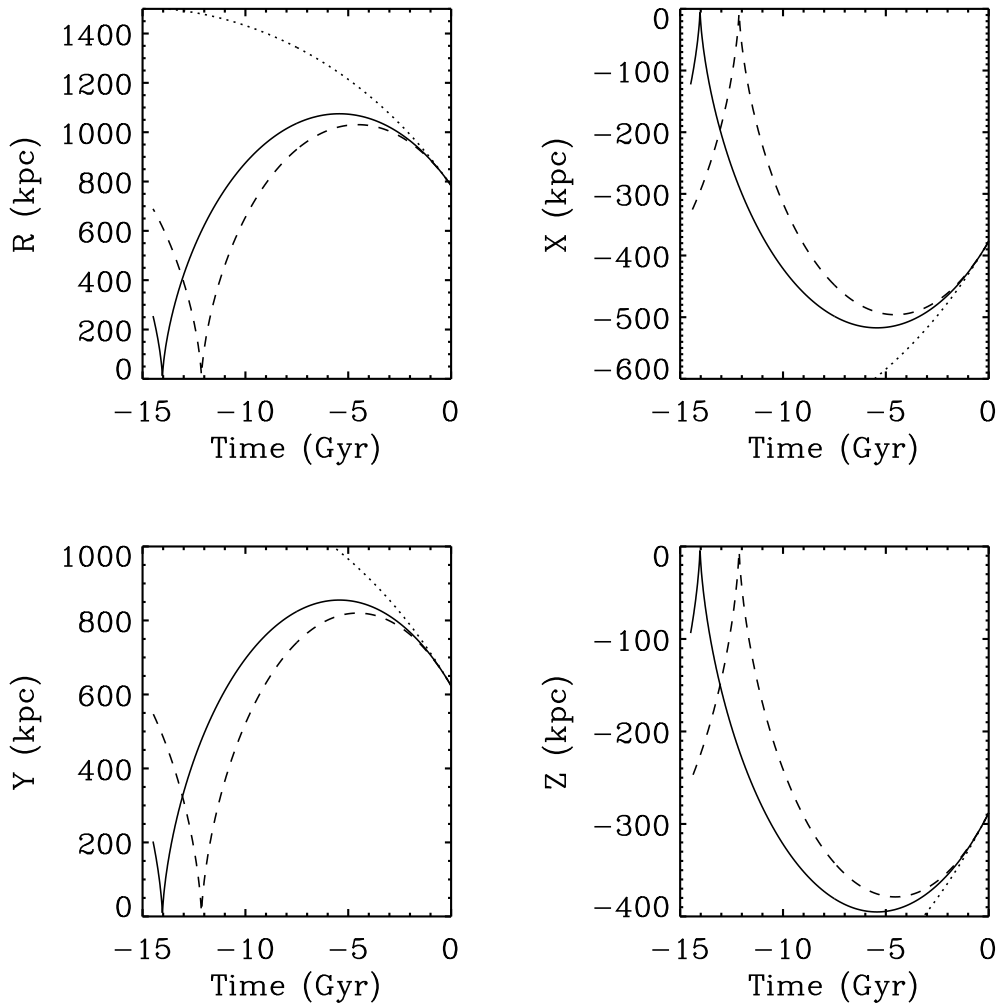

FIG. 1.— The relative orbit of MW and M31 is shown in our Galactocentric X, Y, Z reference frame for a few cases of total mass μ/G. The dotted line shows the past orbit for $\mu/G = 2.6 \times 10^{12} M_\odot$, the dashed line for $\mu/G = 5.2 \times 10^{12} M_\odot$ and the solid line for $\mu/G = 4.6 \times 10^{12} M_\odot$.

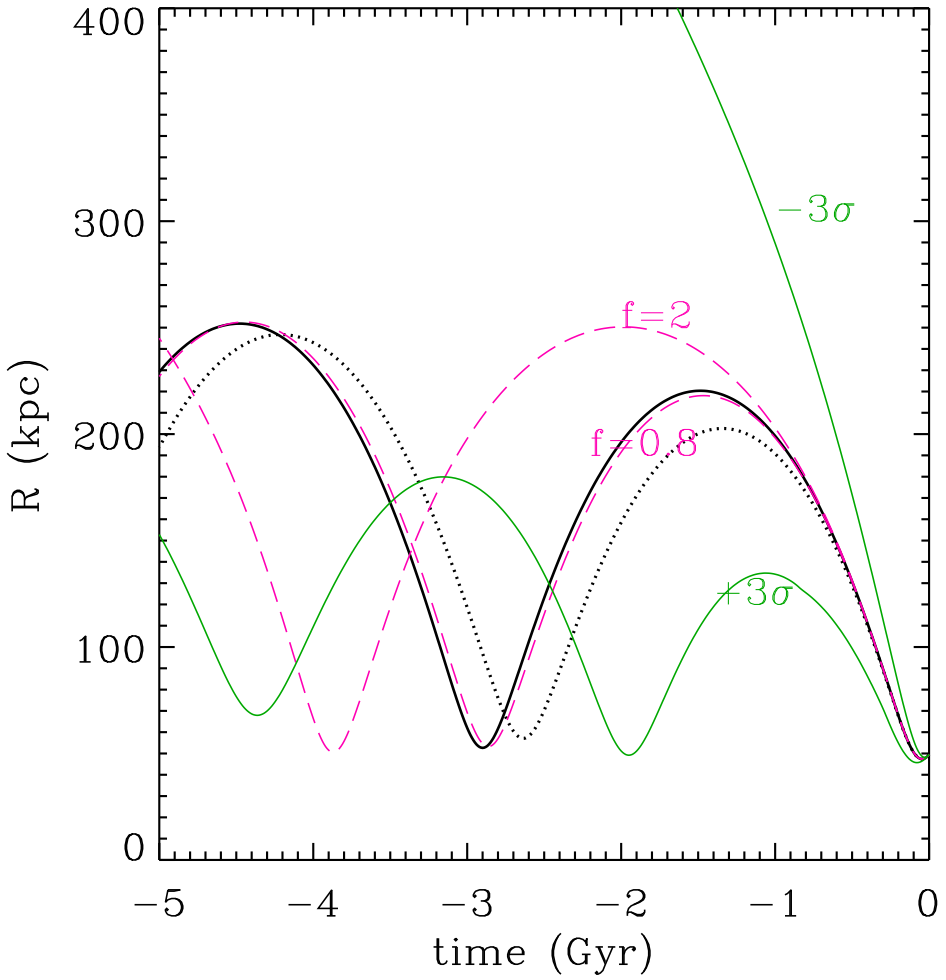

FIG. 2.— The Galactocentric distance of the LMC when M31 is included in the Local Group model ($f = 1$; black solid line) and when it is not (black dotted line). For a given M_{tot}, the pink lines mark the effect of a maximum M31 model ($f = 2$) and a minimum M31 model ($f = 0.8$). The green lines mark the LMC orbit that comes closest to M31, $\sim 3\sigma$ increase in μ_W (marked -3σ), and the furthest orbit, 3σ decrease in μ_W (marked $+3\sigma$).

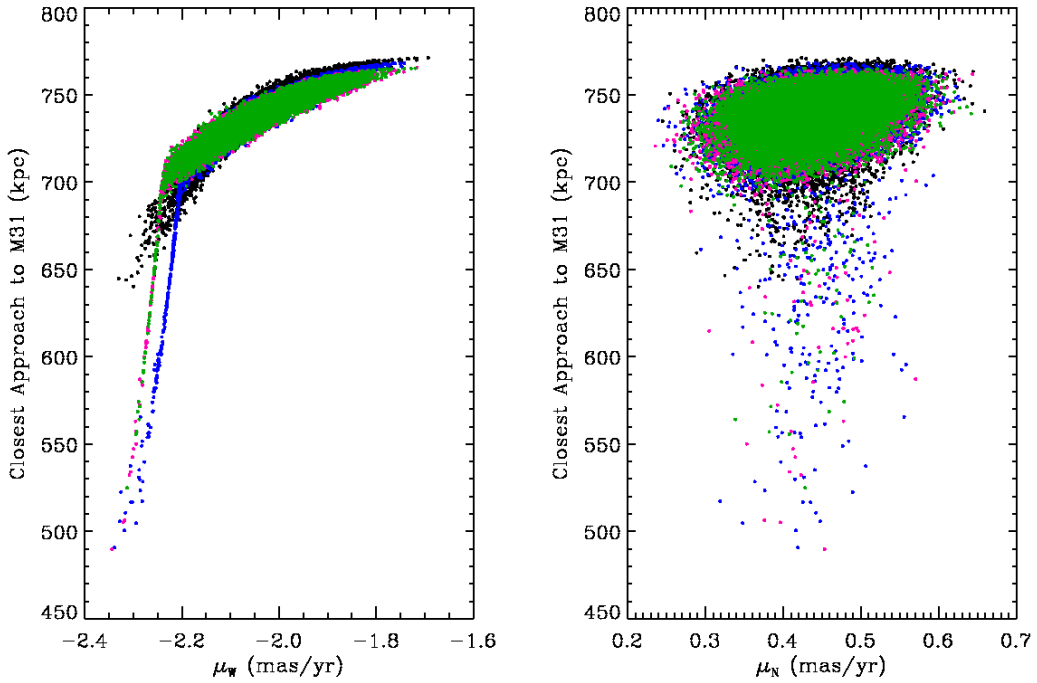

FIG. 3.— The closest approach to M31 as a function of the LMC's μ_W (*left*) and μ_N (*right*). The black dots show the case of $M_{tot} = 2.6 \times 10^{12} M_\odot$, the green dots show $M_{tot} = 3.5 \times 10^{12} M_\odot$, the blue dots show $M_{tot} = 4.6 \times 10^{12} M_\odot$ and the pink dots show $M_{tot} = 5.6 \times 10^{12} M_\odot$.

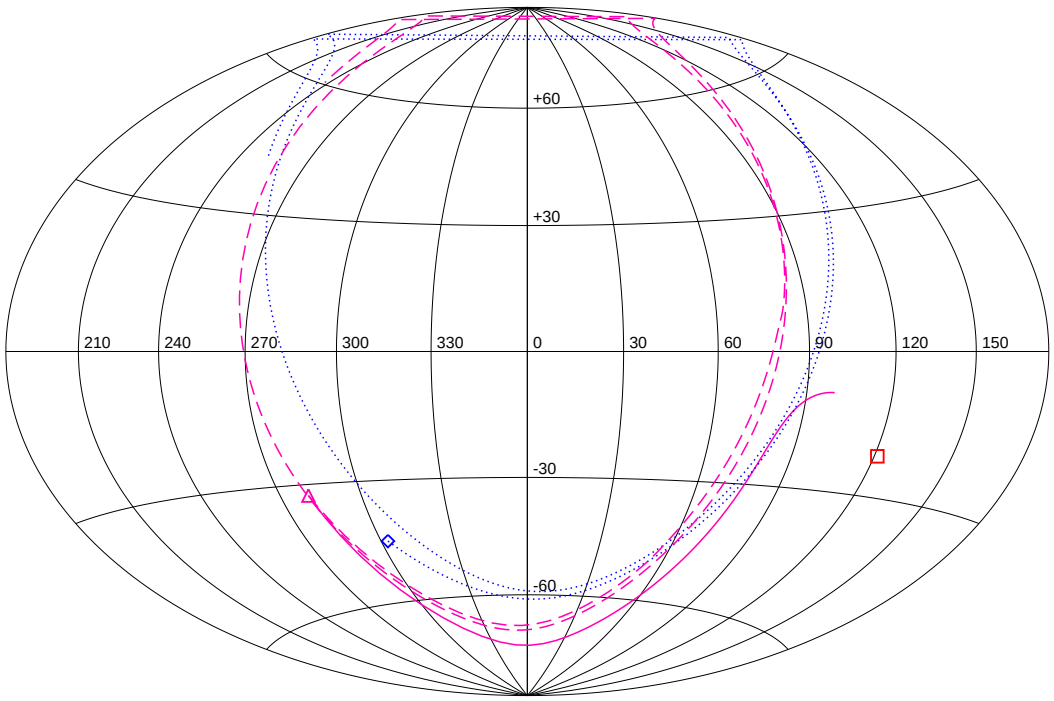

FIG. 4.— The orbital trajectory of the LMC and SMC in aitoff projection for the past 5 Gyr, centered on the MW. The pink triangle, blue diamond and red square mark the current positions of the LMC, SMC and M31 respectively, i.e., at $t = 0$. The pink solid line shows the LMC orbit trajectory that takes it closest to M31 in the past, while the pink dashed lines show the corresponding furthest orbits. The blue dotted line shows the mean SMC orbit.

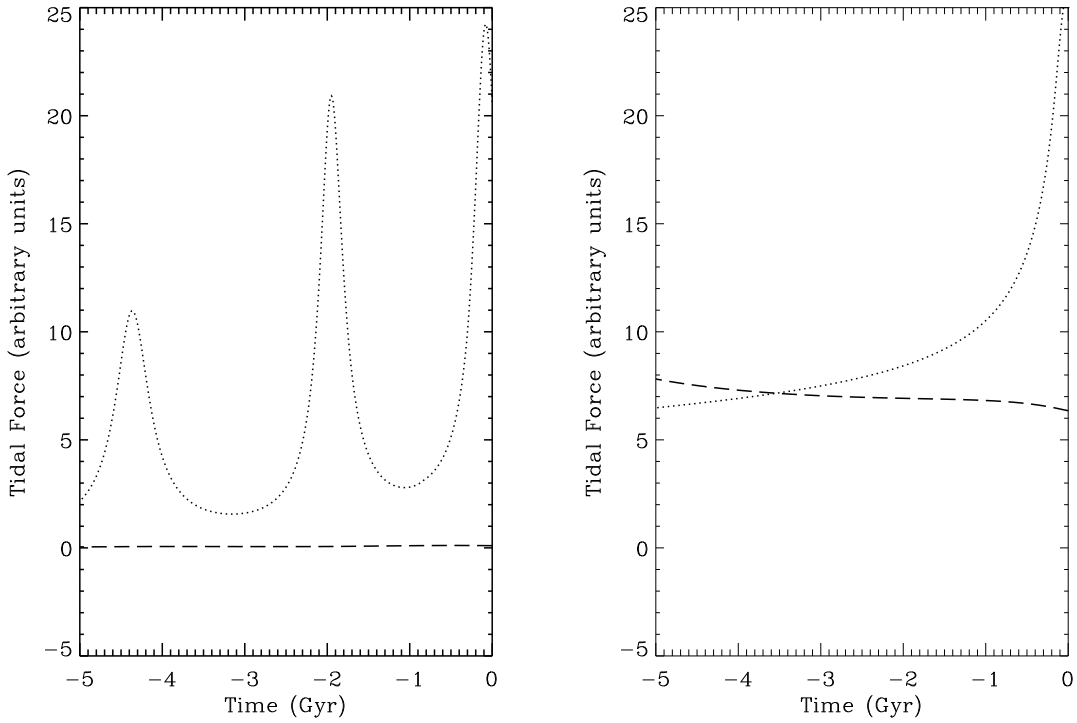

FIG. 5.— The tidal force (in arbitrary units) exerted on the LMC by the MW (dotted line) and M31 (dashed line) as a function of time. (*Left*) The forces on the LMC orbit that is furthest from M31, and (*right*) the forces on the LMC orbit that goes closest to M31.